Experimental Test for Pinned Spins in Ferromagnetic Resonance

R. E. De Wames and T. Wolfram
Science Center, North American Rockwell Corporation, Thousand Oaks, California 91360
(Received 21 July 1970; revised manuscript received 13 May 1971)

The magnetostatic modes of a ferromagnetic film including the uniform mode are *absent* when the spins are pinned and the exchange interaction is included. New modes, the *magnetoexchange* modes, occur with dispersion intermediate between the magnetostatic and exchange dispersions. Formulas and detailed results are presented for both the pinned cases. Experimental tests for deducing the effective boundary conditions are discussed.

Recent ferromagnetic-resonance experiments[1,2] on epitaxial yttrium iron garnet (YIG) films with thicknesses in the micrometer range have shown that both dipole-dominated and exchange-dominated spin-wave modes can be observed in a single high-quality sample.

In order to construct a consistent theory for these resonances it is necessary to consider both dipolar and exchange interactions. Boundary conditions for the time-varying magnetization and/or its normal derivative must also be specified. Two models have been considered extensively in the literature, the pinned and the unpinned models. The magnetization is assumed to vanish at the film surfaces in the pinned model while in the unpinned model the normal derivative vanishes.

We show that when dipole and exchange interactions are included these two models lead to *very different ferromagnetic resonance spectra* for thin films. We show how resonance data may be used to distinguish between the pinned and unpinned conditions. Formulas and detailed results are presented for both models for the perpendicular-field case. It can be shown rigorously that any branch which tends to the frequency of the uniform mode for small wave vectors must also have a magnetization m which is uniform across the film. It is physically obvious that if m is pinned at the surfaces then it must vanish everywhere. On the other hand, at frequencies above the first exchange level a magnetostatic mode can be admixed with a sinusoidal exchange wave to produce a state which satisfies the pinned boundary conditions. This type of branch *must tend to the frequency of the first exchange level when the wave vector tends to zero* and not to the uniform mode frequency. We refer to this new type of branch as a *magnetoexchange* branch. The magnetostatic and magnetoexchange branches are shown schematically in Fig. 1.

For small wave vectors parallel to the surface our results may be summarized as follows:

(1) In the unpinned case the dispersion of the magnetostatic branch is essentially unmodified by the exchange interaction.

(2) In the pinned case the usual magnetostatic branch does not exist. Instead, new types of branches, the magnetoexchange branches, occur with dispersion intermediate between that of the magnetostatic and exchange branches (see Fig. 1).

(3) *The observation of magnetostatic modes below the first exchange mode may be interpreted as conclusive proof that the spins are not pinned.*

(4) The dispersion of ferromagnetic resonance data allows the pinned and unpinned conditions to be distinguished. These results also apply to the case in which the applied field is parallel to the film surface.[3]

We consider here the case of perpendicular resonance in which the applied field H along the z direction is perpendicular to the film surface. The film extends from $z = 0$ to $z = S$ and is infinite in the x and y directions. The details of the general theory[4] have been presented elsewhere so

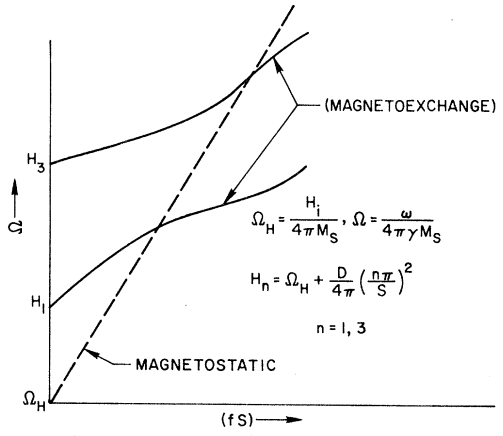

FIG. 1. Comparison of the dispersion of the magnetoexchange modes to the usual magnetostatic mode. f is the wave number parallel to the surface; S is the thickness of the film.

we give only the important results here. The magnetic potential ψ inside the film is an admixture of three waves:

$$\psi = \exp[i(k_x x + k_y y)]e^{-i\omega t} \times \sum_{l=1}^{3} A_l\{\exp(ik_l z) + \eta\exp[-ik_l(z-S)]\}, \quad (1)$$

where $\eta = +1$ and -1 for the even- and odd-symmetry modes, respectively. The requirements of the continuity of the tangential component of $\vec{h}$ and the normal component of $\vec{b} = \vec{h} + 4\pi\vec{m}$ yield the equations

$$\sum_{l=0}^{3}\left[f + k_l\begin{Bmatrix}-\tan(k_lS/2)\\ \cot(k_lS/2)\end{Bmatrix}\right]B_l = 0, \quad (2)$$

where $\tan(k_lS/2)$ $[\cot(k_lS/2)]$ is used with $\eta = +1$ (-1). The quantity f is given by $(k_x^2 + k_y^2)^{1/2}$ and $B_l = [1 + \eta\exp(ik_lS)]A_l$. For small values of f the wave vectors k_l are determined by[4]

$$2y_{1,2} = \Omega - \Omega_H - y_0[2 + \tfrac{1}{2}(\Omega + \Omega_H)]^{-1} \mp [(\Omega - \Omega_H)^2 - y_0(3\Omega_H + \Omega)/(\Omega_H + \Omega)]^{1/2}, \quad (3)$$

$$y_3 = \{(\Omega + \Omega_H) + \tfrac{1}{2}y_0[2 - 1/(\Omega + \Omega_H)]\},$$

where $y_l = [D/(4\pi S^2)](k_lS)^2 = \alpha(k_lS)^2$, $y_0 = \alpha(fS)^2$, and D is the exchange parameter. The quantity $\Omega_H + 1 = H/4\pi M_s$, $\Omega = \omega/4\pi\gamma M_s$; M_s is the saturation magnetization and γ is the gyromagnetic ratio. The wave vector k_1 is independent of α and corresponds to the magnetostatic wave. For $D \equiv 0$ only the k_1 wave is needed for ψ, and Eq. (2) reduces to $f - k_1\tan(k_1S/2) = 0$, which gives the magnetostatic result

$$\Omega = \Omega_H + \tfrac{1}{4}fS + (\text{higher order terms}). \quad (4)$$

For $D \neq 0$ two additional boundary conditions at each surface are required. For the pinned model

$$\sum_{l=1}^{3}\chi_{xx}(k_l)B_l = \sum_{l=1}^{3}\chi_{xy}(k_l)B_l = 0, \quad (5)$$

while for the unpinned case

$$\sum_{l=1}^{3}k_l\chi_{xx}(k_l)\begin{Bmatrix}\tan(k_lS/2)\\ \cot(k_lS/2)\end{Bmatrix}B_l = \sum_{l=1}^{3}k_l\chi_{xy}(k_l)\begin{Bmatrix}\tan(k_lS/2)\\ \cot(k_lS/2)\end{Bmatrix}B_l = 0. \quad (6)$$

In Eqs. (5) and (6) the susceptibilities are given by

$$\chi_{xy}(k_l) = i\Omega[\Omega_H(k_l)^2 - \Omega^2]^{-1},$$
$$\chi_{xx}(k_l) = \Omega_H(k_l)[\Omega_H(k_l)^2 - \Omega^2]^{-1},$$
$$\Omega_H(k_l) = \Omega_H + y_0 + y_l. \quad (7)$$

From Eqs. (2) and (5) we obtain for *small* f the eigenvalue equation for the pinned case[5]:

$$\left[y_0^{1/2} + y_1^{1/2}\begin{Bmatrix}-\tan(y_1/4\alpha)^{1/2}\\ \cot(y_1/4\alpha)^{1/2}\end{Bmatrix}\right] - \epsilon\left[y_0^{1/2} + y_2^{1/2}\begin{Bmatrix}-\tan(y_2/4\alpha)^{1/2}\\ \cot(y_2/4\alpha)^{1/2}\end{Bmatrix}\right] = 0. \quad (8)$$

For $\Omega = \Omega_H + a\sqrt{y_0}$ (which is the functional form for Ω of the magnetostatic branch) the quantity $\epsilon = y_1/y_2$ tends to a constant for small f so that both terms of Eq. (8) are important. If one neglects the second term of Eq. (8) then the spurious solutions are obtained. The solutions for the pinned case are

$$\Omega_p = \begin{cases}H_n + 2fS/(n\pi)^2 & (n = 1, 3, 5, 7, \cdots)\\ H_n + \frac{3}{2}(fS)^2/(n\pi)^2 & (n = 2, 4, \cdots),\end{cases} \quad (9)$$

where $H_n = \Omega_H + \alpha(n\pi)^2$ and provided that $\Omega_H \gg \alpha(n\pi)^2$. The *magnetoexchange* branches corresponding to the odd-integer modes are admixed exchange and magnetostatic modes. These branches begin at $\Omega = \Omega_H + \alpha(n\pi)^2$ and increase with fS with a slope of $2/(n\pi)^2$ whereas the magnetostatic branch [Eq. (4)] begins at $\Omega = \Omega_H$ and has a slope of $\frac{1}{4}$. No solutions to Eq. (8) exist below $\Omega_H + \alpha\pi^2$.

The results for the unpinned case are also determined by Eq. (8) where now

$$\epsilon = (y_1/y_2)^{2/3}\begin{Bmatrix}\tan(y_1/4\alpha)^{1/2}\cot(y_2/4\alpha)^{1/2}\\ \cot(y_1/4\alpha)^{1/2}\tan(y_2/4\alpha)^{1/2}\end{Bmatrix}. \quad (10)$$

The frequencies for the *unpinned* case are

$$\Omega_{un} = H_n + \tfrac{1}{2}(fS)^2/(n\pi)^2 + (D/4\pi)f^2, \quad n = 1, 2, 3 \quad (11)$$

for odd (n odd) or even (n even) exchange branches. In addition there is a magnetostatic branch described by,

$$\Omega_{un} = \Omega_H + \tfrac{1}{4}(fS) + O((fS)^2). \quad (12)$$

Equations (9), (11), and (12) have been confirmed by independent calculations by Walker[6] using a matrix formulation which bypasses the explicit determination of the propagation constants in the medium. The region of validity of Eqs. (9), (11), and (12) is discussed in the latter part of the paper.

In Fig. 2, we present numerical calculations for a YIG film with $M_s = 1750$ Oe, $D/4\pi = 2.6 \times 10^{-12}$ cm^2, and $S = 0.61 \times 10^{-4}$ cm. The applied field is perpendicular to the film surface and has

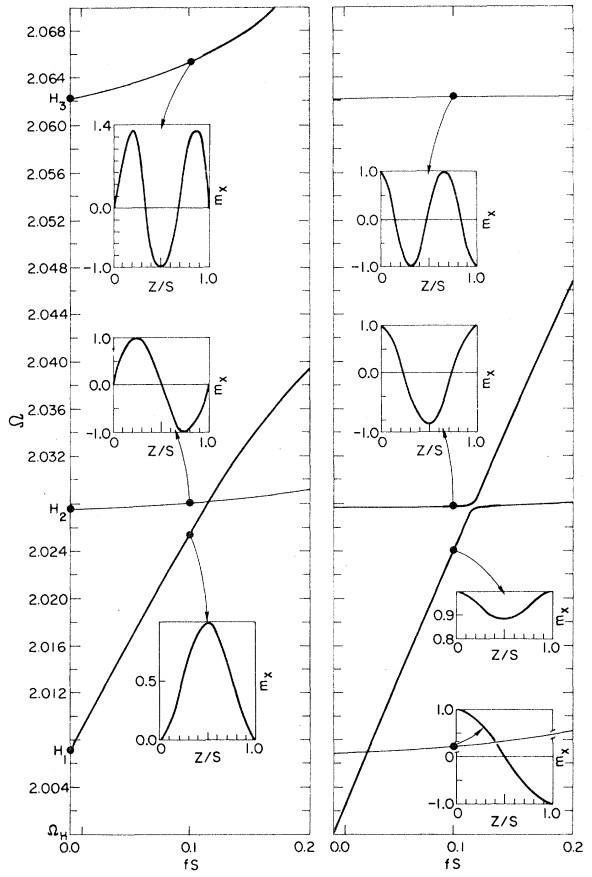

FIG. 2. The left-hand side shows the spectrum and spatial distribution of the magnetization for the pinned conditions. The right-hand side illustrates the spectrum and spatial distribution of the magnetization for the unpinned conditions. The parameters used in the calculation are for YIG. ($D/4\pi = 2.6 \times 10^{-12}$ cm^2, $4\pi M_s = 1750$ Oe, $\Omega_H = H_i/4\pi M_s = 2.0$, and $S = 0.61$ μm). Note the absence of the usual magnetostatic branch below $H_i = \Omega_H + (D/4\pi)(\pi/s)^2$ for the pinned condition.

the value $H = 3(4\pi M_s)$ for which $\Omega_H = 2.0$. The pinned case is shown in the left-hand side of Fig. 2 and the unpinned case on the right. In the pinned case the magnetoexchange level increases linearly from H_1 with a slope of $2/\pi^2 \approx 0.2$. The magnetization eigenstate for the branch at $fS = 0.1$ is shown in the lower insert. It should be noted that the *odd-numbered modes are symmetric* with respect to the center of the film in contrast to the unpinned case shown on the right-hand side of Fig. 2. The admixture of the magnetostatic wave with the even-numbered exchange levels is small. These branches increase quadratically with fS for small values of fS. The admixture with the odd-numbered exchange levels, however, is quite large except at $fS = 0$ where these states are pure exchange states. The magnetoexchange dispersion curve for $n = 1$ not only has a lower slope than the magnetostatic branch but lies lower as fS is increased. In the unpinned case, shown on the right-hand side of Fig. 2, the lowest branch is essentially the same as the magnetostatic branch. The magnetostatic level begins at $\Omega = \Omega_H$ and increases linearly with a slope of 0.25, which is 25% greater than in the pinned case. Mixing of the exchange and magnetostatic waves is large only near a crossover in the unpinned case.

The behavior of the spectra in the pinned and unpinned cases is clearly very different. These differences can be used to determine from experimental data which of the boundary conditions is most appropriate. In a typical experiment on thin films differences of the order of 20 to 30 Oe in the position of the main resonance can be expected. In addition, the experimentally measured shape of the dispersion curves offers a complementary means of deducing the effective boundary conditions. These tests have the great advantage of relying on the resonance frequencies rather than on their intensities.

We conclude with a discussion of the region of validity of Eqs. (9), (11), and (12). First we have established that for finite values of α the slope of the dispersion curve at the origin for the magnetostatic state in the unpinned case is $\frac{1}{4}$, whereas for the first magnetoexchange mode in the pinned case it is $2/\pi^2$. If one sets $\alpha \equiv 0$ in the characteristic equation for the pinned or unpinned case one obtains a slope of $\frac{1}{4}$, but this is a spurious solution in the *pinned* case since for any finite value of α we have rigorously proved the slope at the origin is $2/\pi^2$. Equations (9), (11), and (12) *give the correct behavior provided fS is small enough that the solution does not extend into the crossover region where repulsion between two adjacent branches is important.* This requires that $fS \ll 4\pi^2\alpha$. If α is very small then our solutions are restricted to a small domain of values of fS.

When $\alpha \to 0$ but $\neq 0$ the magnetostatic branch is split into an infinite number of infinitesimal segments which join adjacent exchange branches.[4] In this case it is more appropriate to consider the magnetostatic branch as a virtual state with a finite lifetime due to the interactions with the continuum of exchange states. The results of such a procedure are not yet known.

[1]M. Sparks, B. R. Tittmann, J. E. Mee, and C. Newkirk, J. Appl. Phys. 40, 1518 (1969). See also B. R. Tittmann, Radiat. Eff. 5, 285 (1970).
[2]B. R. Tittmann and R. E. De Wames, Phys. Lett. 30A, 499 (1969).
[3]T. Wolfram and R. E. De Wames, Solid State Commun. 9, 171 (1971).
[4]R. E. De Wames and T. Wolfram, J. Appl. Phys. 41, 987 (1970).
[5]V. V. Gann, Fiz. Tverd. Tela 8, 3167 (1966) [Sov. Phys. Solid State 8, 2537 (1967)].
[6]L. R. Walker, private communication.

Study of Mirror States in $A = 19$ with the (^{6}Li,t) and (^{6}Li,^{3}He) Reactions on ^{16}O†

H. G. Bingham, H. T. Fortune, J. D. Garrett, and R. Middleton
Department of Physics, University of Pennsylvania, Philadelphia, Pennsylvania 19104
(Received 21 April 1971)

The reactions ^{16}O(^{6}Li, ^{3}He)^{19}F and ^{16}O(^{6}Li, t)^{19}Ne have been performed at an incident energy of 24 MeV. The observed strong selectivity of these reactions suggests a predominantly direct-reaction mechanism and allows the identification of several isobaric analogs in ^{19}F and ^{19}Ne.

During the past few years much effort has been devoted to the study of lithium-induced reactions. Most extensively studied have been the α-particle transfer reactions[1-4] (^{6}Li, d) and (^{7}Li, t) and the two-nucleon transfer reaction[2,5-6] (^{6}Li, α). Comparatively few studies have been made of the three-nucleon transfer reactions[2,7] (^{6}Li, ^{3}He) and (^{6}Li, t) until very recently. This lack of interest probably reflected the erroneous belief that the ^{6}Li-induced three-nucleon transfer reactions would be both very weak and unselective. Recent studies,[8] however, have indicated substantial ^{3}He-t clustering in the ^{6}Li ground state. Such clustering is, of course, expected on simple grounds.[9] The present Letter reports preliminary results of a program of (^{6}Li, ^{3}He) and (^{6}Li, t) reactions, demonstrating their use for determining isobaric analogs in mirror nuclei. Ignoring the effects of the Coulomb force, the (^{6}Li, ^{3}He) and the (^{6}Li, t) reactions are expected to be the same. Hence, when these two reactions are studied on self-conjugate targets ($N=Z$), mirror states in the final nuclei would be expected to be populated in a similar manner.

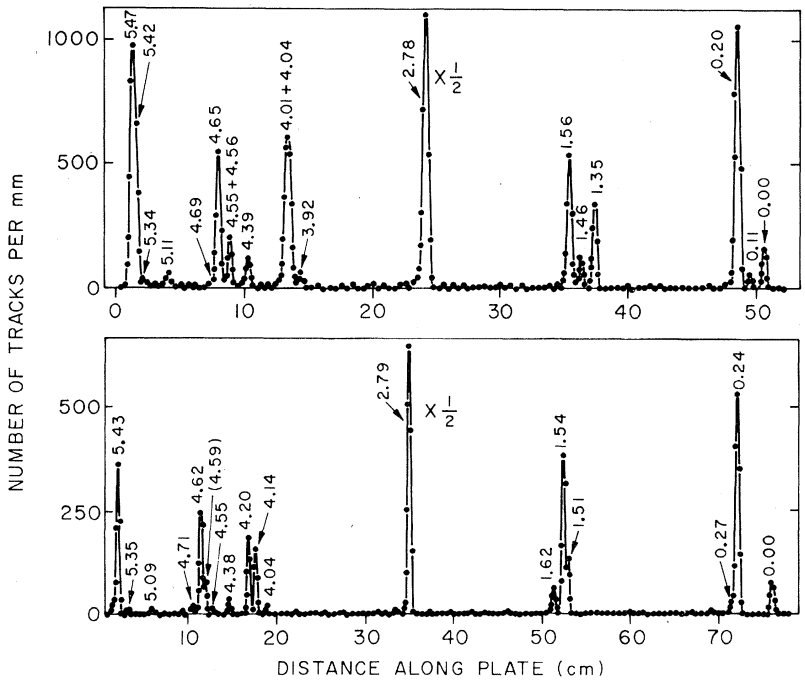

FIG. 1. Energy spectra from the reaction ^{16}O(^{6}Li, ^{3}He)^{19}F (top) and the reaction ^{16}O(^{6}Li, t)^{19}Ne (bottom). Both spectra were obtained at a laboratory angle of 7.5 deg with a 24-MeV incident ^{6}Li beam.